Chapter 2

Clay Minerals and Clay Mineral Water Dispersions — Properties and Applications

Guadalupe Sanchez-Olivares, Fausto Calderas, Luis Medina-Torres, Antonio Sanchez-Solis, Alejandro Rivera-Gonzaga and Octavio Manero

Additional information is available at the end of the chapter

http://dx.doi.org/10.5772/61588

Abstract

This chapter deals with the properties and applications of clay mineral water dispersions and clay minerals as flame retardant additives for polymers. Clay minerals, such as kaolinites, micas, and smectites, are the basic constituents of clay raw materials, which are classically employed in the ceramic industry to produce porcelain, fine ceramics, coarse ceramics, cements, electro-ceramics, tiles and refractories. These products are mainly used in sectors of economic importance, such as agriculture, civil engineering, and environment. A direct method to prepare clay mineral polymer composites is through dispersion in water. Water dispersions of clay exhibit some interesting flow phenomena such as yield stress; i.e., the material behaves as a solid until a critical force applied on the material forces it to flow. Water dispersions of clay have also been reported to be used to prepare materials with enhanced flame-retardant properties such as leather. On the other hand, direct melt compounding of clay mineral with different polymers as the composite matrix (HIPS, PP, and HDPE) to prepare a number of polymer composites with flame-retardant properties has also been reported.

Keywords: Clay minerals, ceramics, polymer nanocomposites, clay water suspensions, flame-retardant leather

1. Introduction

Clay minerals have recently been one of the most used materials in many research and development areas. Clay minerals are excellent as clarifiers, absorption and adsorption materials. They are used in many industrial applications such as paper, paint, petroleum, ceramic, cement, adhesive, asphalt, and food and health-care industry due to their versatility, abundance, and low cost [1, 2].

Currently, clay minerals have been proved to have a wide range of new applications, specifically as reinforcing agents of polymers to produce nanocomposites. Nanocomposites are high-performance composite materials in which one of the phases that compose them has dimensions in the nanoscale (10^{-9} m). The surface area-to-volume ratio of the reinforcing materials contained in a nanocomposite is of paramount importance and plays a key role in the final properties of these materials [3]. Clay minerals, and specially smectites, are materials that offer a high area-to-volume ratio (layered silicates) to be used as reinforced agents in polymer matrices [3–9]. Smectites contain not only external surface but also internal surface, and after a certain treatment, this internal surface can absorb the hydrophobic molecules of organic compounds [10]. The high surface area-to-volume ratio is maximized when the individual platelets, naturally occurring as stacks, become delaminated (exfoliated), thus offering large-scale interactions as reinforcing materials. The thickness of individual platelets (layers) is about 1 nm. Other important reinforcing agents for preparing polymer nanocomposites are carbon nanotubes (CNTs) [11] and, more recently, graphene [12, 13].

Many of the properties that clay minerals impart on polymer nanocomposites are due to the exfoliation and good dispersion of clay platelets which are initially in stacks. A direct method to prepare clay mineral composites is dispersion in water which has been used as an initial approach to produce clay–polymer composites [14]. Water dispersions of clay also exhibit some interesting flow phenomena such as yield stress; i.e., material behaves as a solid until a critical force applied on the material forces it to flow. These clay dispersions have been used as model fluids to study complex flow phenomena and to test some rheological constitutive equations predictions [15]. Water dispersions of clay minerals have also been used to prepare materials with enhanced flame-retardant properties such as leather [16].

Clay–polymer nanocomposite properties mainly depend on the type of clay mineral, chemical modification, concentration, dispersion, structure, and process conditions. With respect to chemical modification of clay minerals, this step has been proven to be crucial in preparing flame-retardant polymer materials. Chemical modification of clay minerals can either produce an effective halogen-free flame-retardant material or, on the contrary, causes a negative effect and increases polymer flammability. In high-impact polystyrene (HIPS), both natural and modified sodium montmorillonite (Na^+Mt) were used to study the burning rate of the nanocomposite produced. It was found that when natural Na^+Mt is added to HIPS, an antagonistic effect on the burning rate is observed: the burning rate increases with respect to virgin HIPS. However, when triphenyl phosphite-modified sodium montmorillonite is added (at a specific content) to HIPS, the burning rate is effectively reduced [17].

Process conditions have an important impact on polymer nanocomposites properties [18]. It is necessary to find the appropriate processing conditions in order to disperse clay minerals at the nanometric level. The effect of processing conditions on HIPS, polypropylene (PP) and high-density polyethylene (HDPE) using modified Na^+Mt and bentonite has been reported [19–21]. Two different extrusion processes were applied: twin extrusion and single extrusion adapted with a special static mixer die and with and without on-line ultrasound application. For HIPS composites, it was found that when the static mixer die is employed, the heat release rate of HIPS is reduced attributed to better clay dispersion. With regard to HDPE and PP, when

on-line ultrasound is applied, modified clay mineral (at specific content) is dispersed effectively (presumably at the nanometric level) and mechanical properties, Izod impact resistance, tensile strength, strain at break, and tenacity were also improved. It was also possible to optimize the content of flame-retardant additives with respect to traditional polymer composites; the materials were classified as V0 (burning stops within 10 seconds on a vertical position specimen; drips of particles allowed as long as they are not inflamed) in accordance with the UL94 standard (ASTM D3801).

To produce nanocomposites, not only polymer matrix materials are used but also metal and ceramic-based materials have been reported [3]. Traditional ceramics have good wear resistance and very high thermal and chemical stability properties. Their main disadvantage for many potential industrial applications is their brittleness. Ceramic-based nanocomposites have recently received attention to produce ceramics with higher performance as the incorporation of reinforcing agents in the form of whiskers, fibers, platelets, and particles to render ceramics with improved fracture toughness. Among the reported reinforced agents used for ceramics are CNTs [22, 23] and graphene [24].

Clay minerals, such as kaolinites, micas, and smectites, are the basic constituents of clay raw materials. The latter are classically employed in the ceramic industry to produce porcelain, fine ceramics, coarse ceramics, cements, electro-ceramics, tiles, and refractories [10, 25]. These products are mainly used in sectors of economic importance, such as agriculture, civil engineering, and environment.

This chapter deals with the properties and applications of clay mineral water dispersions (subchapter 2) and clay minerals as flame-retardant additives for polymers (subchapter 3). Subchapter 2 is divided into three sections: the first one is dedicated to discuss yield stress phenomena (subsection 2.1), the second one discusses the use of an unmodified clay mineral (Na^+Mt) water dispersion as a precursor to prepare an epoxy resin-based composite (subsection 2.2), and the last one deals with the application of clay mineral dispersions to prepare leather with flame retardancy properties (subsection 2.3). Subchapter 3 is also divided into three sections to give examples of clay mineral polymer composites based on different polymers: HIPS (subsection 3.1), PP (subsection 3.2), and HDPE (subsection 3.3), where good dispersion of clay mineral and additives in the polymer matrix is proved to be a key issue in preparing this type of materials.

2. Clay mineral water dispersions

Clay mineral dispersions have a wide range of applications in the industry. For example, they are used as prominent excipients in the pharmaceutical industry to impart adequate semisolid formulations [26]. Rheology is very important in this type of materials, since a correct understanding of their flow properties allows improvement and optimization of the processing conditions and characteristics of the final products. Aguzzi et al. [27] studied the thixotropy in peloid systems (concentrated clay suspensions in mineral medicinal water). Cruz et al. [28] studied the rheological properties of bentonite and kaolinite dispersions in copper–gold

flotation systems. They also discuss the yield stress phenomena exhibited by kaolinite dispersions and how pH affects the Bingham yield stress of these systems and the diverse configurations that the kaolinite platelets adopt related to this phenomenon. The viscoelastic behavior and yield stress of clay mineral dispersions (smectites, beidellite, and montmorillonites) have also been reported by Paineau et al. [29]. Also aqueous clay mineral dispersions are employed as precursors to prepare composites and nanocomposites of which epoxy resin nanocomposites are of special interest here, specifically when the clay mineral used is not organically modified. More recently, clay minerals have been used for the preparation of materials with flame-retardant properties such as leather, which would allow direct incorporation of flame-retardant additives on-line, instead of treating the finished leather with spraying methods. Flame-retardant leather can be used as upholstery material in aeronautic and automotive applications.

2.1. Yield stress in water clay dispersions

The yield stress of clay mineral water dispersions has received a lot of attention [15, 28, 29]. The yield stress phenomenon occurs when the shear stress does not depend on the shear strain (constant value). Under these circumstances, the system behaves as an elastic solid. However, upon increasing the strain rate, after a critical point is reached (yield stress), the material starts to flow. The "real" yield stress has been associated with the Bingham yield stress, i.e., an asymptotic nonzero value of the stress as the shear rate tends to zero. While the term "apparent yield stress" is associated with a very large zero-shear rate viscosity, which corresponds to a zero shear viscosity plateau. A viscoplastic material under strain exhibits little or no deformation up to a critical value of stress which is called the yield stress. Above this critical point, the material starts to flow. Concentrated dispersions of solid particles in Newtonian liquids (such as aqueous clay mineral suspensions) exhibit yield stress followed by nearly Newtonian behavior. These materials are often called Bingham plastics. Various other fluids of a practical interest, such as liquid foams, paints, droplet emulsions, or high cholesterol blood, possess such elastoviscoplastic behavior.

Cheng [30] reported that the stress becomes almost independent of the shear rate in an intermediate range of shear rates, while increasing shear rates results in Newtonian-like behavior. The presence of an essentially horizontal region in a double logarithmic plot of stress versus strain rate has been considered to be the most satisfactory criterion for the existence of a yield stress [31]. Regarding rheological models that predict yield stress at moderate shear rates, both the Bingham [32] and the Herschel–Bulkley [33, 34] models predict a flattening of the stress as a function of shear rate. One of the computational problems mentioned by Barnes [32] is that the behavior of a Bingham or similar materials at the yield stress is in no way smooth and differentiable in a mathematical sense. At stresses below the yield stress, the viscosity becomes indefinite (tending to infinite). At stresses above the yield stress, the viscosity is an asymptotically decreasing function of shear stress, usually tending to a constant value of viscosity as the stress becomes infinite. These problems can lead to inconsistencies in the numerical modeling of flow in complex geometries, and difficulties in properly defining the boundaries between nondeforming "solid" zones and flowing "liquid" zones.

http://dx.doi.org/10.5772/61588

Several constitutive equations have been proposed to model yield stress phenomena: Papanastasiou [35] proposed a slightly modified version of the Bingham plastic [33], containing three fitting parameters. Although this model is continuous and differentiable, it does not predict a real solid-like behavior. Alternative models have been proposed to account for the real solid case (Hookean behavior before yielding). Houlsby and Puzrin [36] and Isayev and Fan [36] proposed models which are based on the original Voigt-Kelvin or Maxwell-like behavior with added yield stress terms. The Houlsby and Puzrin [36] model predicts an elastic behavior before yielding, and a Kelvin–Voigt solid behavior at long times (after yield), while the Isayev model [37] predicts a Hookean elastic behavior before yielding and a viscous one after yielding. These models have the disadvantage that the solid–liquid transition is discontinuous. Saramito [38, 39] proposed a constitutive equation for elastoviscoplastic materials which is continuous and differentiable. Nevertheless, it does not predict a real solid-like behavior. To predict a solid behavior, a new version of the latter viscoplastic model was suggested, based on the Herschel–Bulkley one [34]. In summary, models that predict real solid behavior and a smooth transition to liquid-like behavior are mostly empirical. Bautista et al. [40] presented a model (Bautista–Montero–Puig [BMP] model) that predicts several rheological phenomena observed in complex materials. This model has been shown to describe the apparent and real yield stress behavior [15].

Fig. 1 shows a log–log plot of the stress versus shear rate for various values of the fluidity φ_0 (inverse of the viscosity function $1/\eta_0$). In the case of $\varphi_0>0$, the stress goes to zero as the applied shear rate goes to zero, except when $\varphi_0 = 0$; in this case, Bingham behavior is observed, corresponding to a real yield stress. In the inset, the linear plot depicts the region of very small shear rates, showing that all the curves tend to zero, except curves I, II, and III. Although these curves show a real yield stress, only curve I fulfills the term "real," since curves II and III show an "apparent" yield. This is only observed in the linear plot (inset) where the stress reaches the true yield stress value at zero rate of deformation (y-intercept).

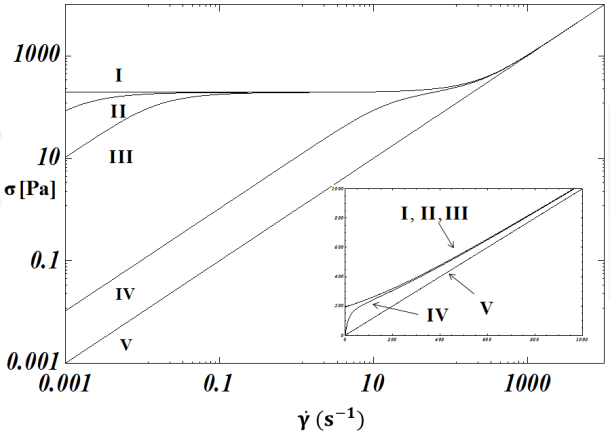

Figure 1. BMP model predictions of the shear stress as a function of shear rate (log–log plot) for various values of the zero shear-rate fluidity. As this parameter tends to zero, the real yield stress is reached. Inset: Linear plot.

Fig. 2 shows predictions of the BMP model for the velocity profile (radial position from lower pipe wall $r/R = 0$ to upper pipe wall $r/R = 1$ versus axial velocity V_z) of a general fluid flowing in a pipe of normalized diameter (pipe of length $z = L$ and radius $r = R$), i.e., Poiseuille flow. In the simulations II–V, the shape of the velocity is parabolic. Under Poiseuille flow, when the flow becomes more and more dominated by the yield stress, the velocity profile becomes more plug-like (zero velocity case I, Fig. 1). This arises because the material deformation is restricted in the tube to just near the wall.

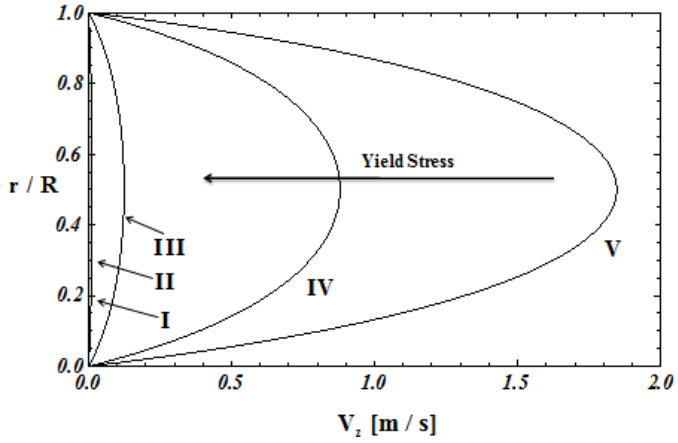

Figure 2. BMP model predictions for the velocity profile of pressure driven flow of a complex fluid with approximating from the no yield stress case (V) to the real yield stress case (I) in a circular pipe.

The BMP model possesses the capacity of predicting the rheological behavior of complex structural fluids such as wormlike micellar solutions, dispersions of lamellar liquid crystals, associative polymers, bentonite suspensions, polymer-like micellar solutions, and polymer nanocomposites [40–48]. In addition, the model reproduces the complete flow curve for a shear-thinning and shear-thickening fluid, i.e., Newtonian plateau at low and high shear rate, and the intermediate power law region for viscosity, and nonvanishing normal stress difference. The model also gives a reasonable description of the elongational and complex viscosity with finite asymptotic value and non-exponential stress relaxation and start-up curves, thixotropy, and shear-banding flow. Yield stress predictions for this model have been proved to be in very good agreement with rheological data at short times (steady and unsteady state measurements) for kaolin (a clay mineral) suspensions in water at 60% mass concentration and also for ketchup [15]. The one-mode model fails to predict the behavior for these materials at long times. A more recent version of the model has been proposed as a linear sum of modes. Such model is more effective in modeling the behavior of complex materials at long times [49].

Fig. 3 shows a comparison of different model predictions in the yield stress region. The "real" yield stress models in Fig. 3 predict an asymptotic region independent of the shear rate for shear rate tending to zero [33, 34, 40, 50]. In the insets, models that predict "apparent" yield

http://dx.doi.org/10.5772/61588

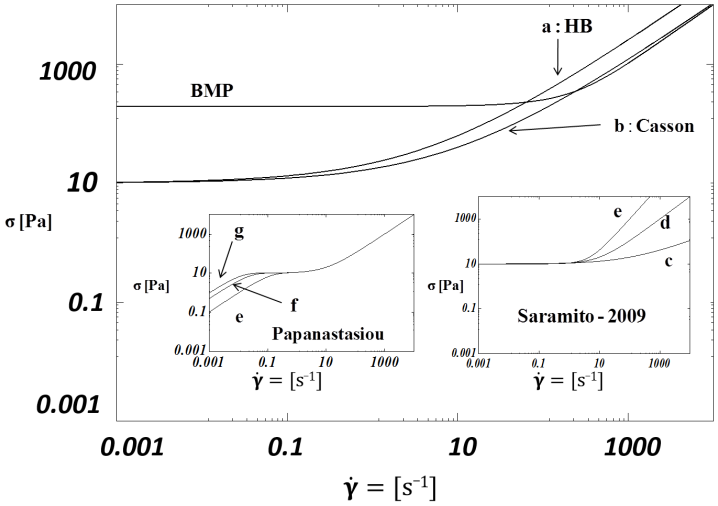

Figure 3. Shear stress versus shear rate showing various model predictions. Parameters for the simulations are as follows: Herschel–Bulkley, n = 0.5, σ_y = 10. Saramito n = 0.5, 1.0, 1.5, σ_y = 10. Casson, σ_y =10. Bingham, σ_y =10. Papanastasiou, n = 5, 10, 15, σ_y = 10. BMP, σ_y =26.

stresses illustrate the region at vanishing shear rates where the flow curves tend to a very high zero-shear rate viscosity [35, 38]. The BMP model predicts characteristic rigid solid behavior before yielding of the Bingham [33] or Herschel–Bulkley [34] models applicable for an elastic or viscoelastic solid behavior, as in the Houlsby and Puzrim [36], Isayev and Fan [37], or Saramito [38, 39] models. Finally, after yielding, it predicts either a shear thickening, a shear thinning, or a Newtonian behavior [40].

2.2. Composites with clay mineral water dispersion as precursor

There are a large number of reports about clay mineral thermostable resin nanocomposites. However, most of these studies deal with epoxy–silicate systems rather than sodium montmorillonite (Na^+Mt)–polyester systems. Furthermore, montmorillonite is organically modified in order to be used in epoxy- and polyester-based nanocomposites [51–55]. There are few studies regarding unmodified montmorillonite which is basically used to compare with the organically modified one. Unmodified montmorillonite is incompatible with the polymer due to its hydrophilic nature. Attempts to use suspensions of mineral clay as a precursor to prepare thermostable resin nanocomposites are even scarcer. For example, it has been reported that the hydrated form of the Na^+Mt facilitates the intercalation of an epoxy monomer in the clay interlaminar spacing. When hydration of clay occurs, the platelets of Na^+Mt separate from each other as the forces of layers attraction weaken due to water entering the interlaminar spaces [56]. Clay montmorillonite suspensions have been used to prepare exfoliated nanocomposites by mixing it with melt polymer (nylon 6). The high temperature of the melt polymer evaporates the water, leaving the final polymer matrix with regions of exfoliated clay as well as tactoids

of clay [57]. A slurry compounding method has also been reported. Na^+Mt is suspended first in water and then ketone or alcohol is added to form a binary system. Then, the montmorillonite is treated with xylane to obtain modified clay. This modified clay is used to produce epoxy–nanoclay systems [57–59].

A more recent attempt in the preparation of unsaturated polyester resin nanocomposites is based on an unmodified mineral clay suspension in water as a precursor [14]. Na^+Mt is suspended in water (Na^+Mt/H_2O) to incorporate this suspension in an isophtalic neopentylic polyester resin (UP) which is then polymerized. Clay mineral individual layers are separated in the aqueous suspension and allows the resin molecules to intercalate in the interlayer spacing. The mixing method and clay mineral/water proportion are key features in the preparation of this nanocomposite. In this case, a 1:1.5 (water-to-clay) proportion was used, which is lower than what is reported in the literature.

UP nanocomposites obtained by this method (clay mineral water suspension) showed augmented mechanical properties in comparison with UP resin without clay and UP-Na^+Mt resin with unsuspended clay mineral at a concentration of 5 phr mineral clay. Flexural strength and flexural modulus values showed increments of 13% and 120%, respectively, for the suspended clay–resin system as compared to the UP resin, see Table 1.

Na^+Mt concentration [phr]	UP-Na^+Mt		UP-Na^+Mt/H_2O	
	Flexural strength [MPa]	Felxural modulus [MPa]	Flexural strength [MPa]	Felxural modulus [MPa]
0	31.3 (±0.2)	830 (±8)	31.3 (±0.2)	830 (±8)
1	33.4 (±0.6)	884 (±4)	41.3 (±0.9)	1296 (±93)
3	36.7 (±1.1)	905 (±66)	30.0 (±1.1)	959 (±10)
5	39.8 (±0.9)	1189 (±44)	35.5 (±1.2)	1821 (±15)

Table 1. Flexural strength and flexural modulus for samples UP-Na^+Mt and UP-Na^+Mt/H_2O.

These increased values are attributed to the intercalation of the resin in the interlayer space of the clay platelets. This intercalation enhances the polymer-clay interaction and the stress distribution, transferring the polymer matrix stresses to the nanoclay platelets, and improving the mechanical properties. Intercalation of the polymer in the clay platelets was evidenced by X-ray diffraction pattern, where the basal spacing of the platelets Na^+Mt (1.23 nm) was incremented at UP-Na^+Mt/H_2O to 1.56 nm [14]. Clay mineral intercalation was further evidenced by transmission electron microscopy (TEM) and scanning electron microscopy (SEM) techniques. Fig. 4 shows a TEM micrograph of arrangements of three, five, and six intercalated platelets in the UP matrix; the platelets show no exfoliation at all. SEM micrographs in Fig. 5 shows the fractured surface of the nanocomposite (Fig. 5b), which is more rugged than the surface of the UP matrix alone (Fig. 5a), and indicates the existence of bonds between the clay mineral and the polymer matrix.

http://dx.doi.org/10.5772/61588

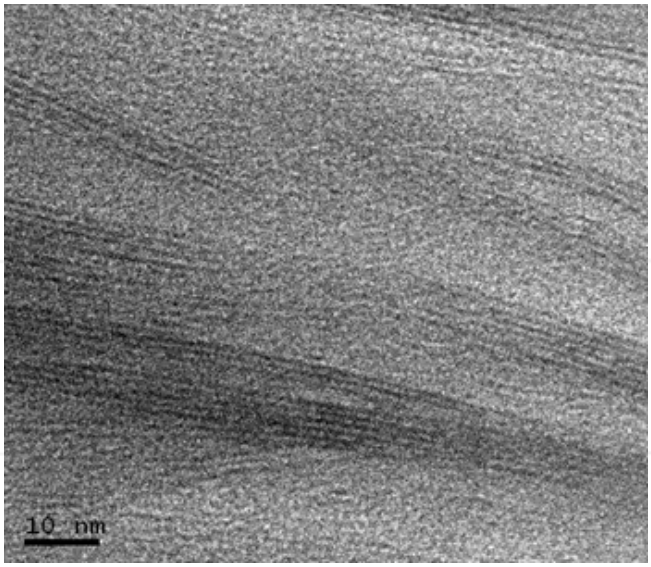

Figure 4. TEM micrograph showing sample UP-Na^+Mt/H_2O. The polymer matrix is intercalated in the interlaminar space of the clay platelets which preserve an ordered configuration.

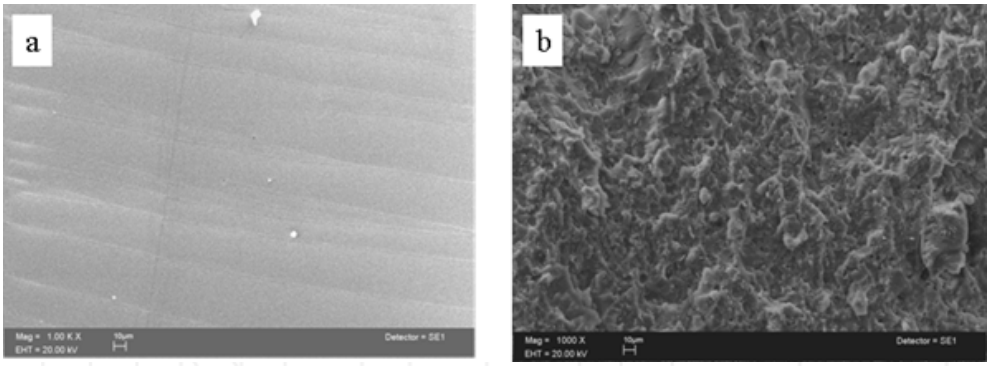

Figure 5. SEM micrographs for UP (a) and UP-Na^+Mt/H_2O at 5 phr clay content (b).

Thermogravimetric analysis (TGA) revealed that the nanocomposite UP-Na^+Mt/H_2O is more resistant to degradation than UP polymer (Fig. 6) with the unsuspended clay mineral sample (UP-Na^+Mt) in the middle of them. This is attributed to the intercalated clay platelets which act as a thermal insulator and as a mass transport barrier.

Rheological analysis evidenced a shift in the gelation temperature toward higher temperatures, from 86°C for UP to 96°C for UP-Na^+Mt/H_2O sample (5 phr of suspended Na^+Mt) (Fig. 7). Sample with non-suspended Na^+Mt showed an intermediate gelation temperature (92°C).

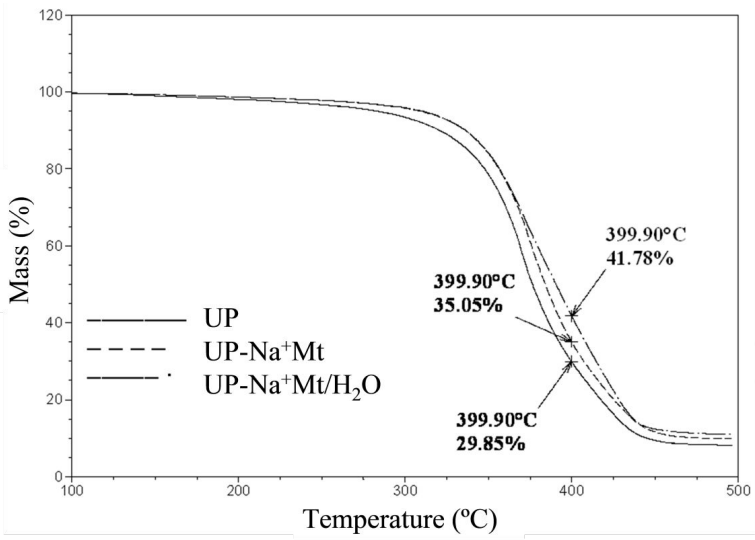

Figure 6. Mass loss from TGA analysis for UP, UP-Na^+Mt/H_2O 5 phr clay, and UP-Na^+Mt 5 phr clay.

When Na^+Mt acquires an intercalated structure within the polymer matrix, an interconnected network is formed which, in principle, is more thermally stable and caused an increase in the gelation temperature.

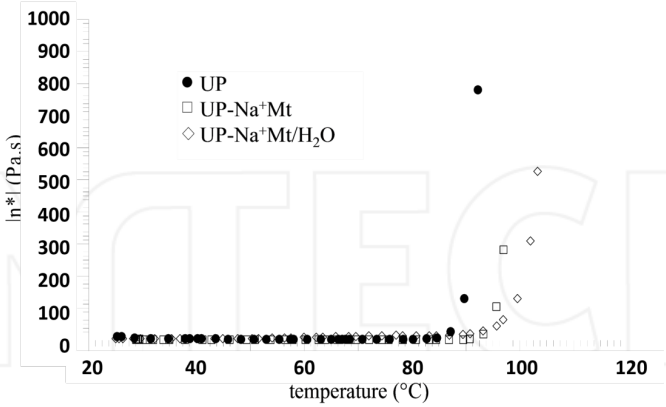

Figure 7. Complex viscosity versus temperature for samples UP, UP-Na^+Mt 5 phr clay and UP-Na^+Mt/H_2O 5 phr clay mineral where gelation temperature is evidenced as a sudden increase in viscosity.

Regarding continuous shear flow, shear viscosity data revealed an increase for UP-Na^+Mt/H_2O of almost two decades in comparison with pure UP together with a shift from Newtonian to

http://dx.doi.org/10.5772/61588

a strong shear thinning behavior and a tendency towards a yield stress value at low shear rates. The interconnected network formed by the intercalated structure is destabilized by shear, which is evidenced by superimposed viscosity curves at high shear rate (Fig. 8). Unsuspended Na^+Mt has little or almost no influence in the rheology of the system with the water added acting only as a lubricant by reducing the viscosity of the sample.

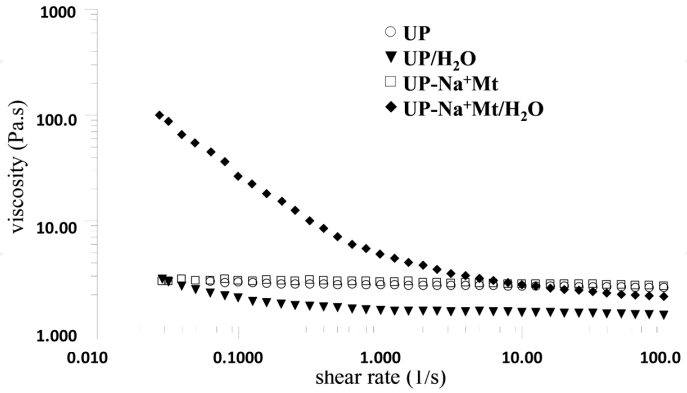

Figure 8. Shear viscosity for the systems UP, UP/H_2O, UP-Na^+Mt 5 phr clay, and UP-Na^+Mt/H_2O 5 phr clay.

Frequency sweep measurements in the linear viscoelastic regime performed on the uncured samples are presented in Fig. 9, the system UP-Na^+Mt/H_2O revealed characteristics of a weak gel with storage modulus (G') values independent of the frequency applied, while samples UP and UP-Na^+Mt (unsuspended clay) showed a viscoelastic liquid behavior, i.e., slope values of ~1 and 2 for G' and G'', respectively, at low frequencies.

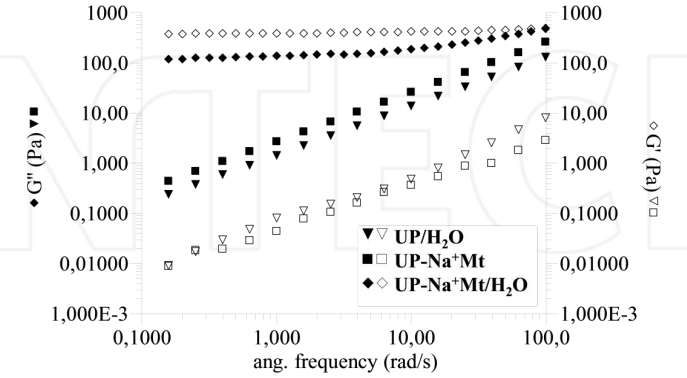

Figure 9. Storage and loss moduli versus frequency from linear viscoelastic measurements for samples UP, UP/H_2O, UP-Na^+Mt 5 phr clay, and UP-Na^+Mt/H_2O 5 phr of clay.

2.3. Clay mineral as flame retardant for leather

In recent years, the tannery industry has paid attention to clay minerals because of the potential advantages that these materials represent. Research works about the use of clay minerals on leather have reported better leather performance on processes such as tanning, coating, and, ultimately, in the final properties of the leather itself [60]. Nevertheless, reports on leather flame-retardant properties using clay minerals are still rare. In spite of this, clay minerals have shown very good synergistic effect on flame-retardant properties. A considerable reduction on the content (load) of flame-retardant additives (other than clay minerals) in polymer composites has been reported by using clay minerals [20, 21].

The effect of sodium montmorillonite (Na^+Mt) on the morphology, thermal, flame-retardant, and mechanical properties of semi-finished leather was studied in order to obtain flame-retardant leather for upholstery uses in the aeronautic industry [16]. In this investigation, Na^+Mt particles were dispersed in hot water at 1:20 ratio (Na^+Mt:water), along with continuous stirring. This dispersion was incorporated into the leather during an ordinary retanning process in a drum, as it is commonly used in the tannery industry. Dispersion of Na^+Mt and leather was rotated for a specific time. Three samples with different Na^+Mt contents of 1, 3, and 6 wt.% were prepared.

Leather morphology was studied by scanning electron microscopy (SEM). Sample reference (leather without Na^+Mt) showed a grain surface with different pore sizes (from 100 μm to 400 nm). The cross section showed interstitial voids between fibers of leather. Based on the leather morphology, we can assume that the Na^+Mt particles penetrate inside the leather through the pores during the retanning process. Mapping of elements (Si, Al, and Mg) was carried out on the leather samples with the different contents of Na^+Mt. The elements mapping pointed out that Na^+Mt particles were well distributed and dispersed within the leather structure.

Thermal stability of the leather samples was studied by thermogravimetry. The test analysis in nitrogen atmosphere showed that leather degrades in a single stage, with a maximum degradation temperature of 327°C. However, when leather degrades in atmospheric air, the degradation mechanism presents two main stages. The first stage occurs at a maximum degradation temperature of 319°C and the second one at 459°C. The mass loss of the leather in both test analysis is attributed to the collagen, since it is the main component of leather [61, 62]. Clay mineral inside the leather changes the thermal degradation mechanism. According to test analysis, leather with Na^+Mt samples exhibited better thermal stability than the reference sample (without clay mineral).Particularly at the second stage, the maximum degradation temperature of the leather with Na^+Mt samples increased to 469, 463, and 463°C at 1, 3, and 6 wt.% of Na^+Mt.,

Flame-retardant properties were evaluated through a 60-second vertical flammability test according to "14 C.F.R. (code of federal regulations) F part 25 title 14—aeronautics and space, published by United States of America transportation department." According to Table 2, Na^+Mt particles significantly improved the flame-retardant properties of semifinished leather. The burning length of leather was reduced from 16.4 cm to 13.3 and 13.4 cm for samples with 3 and 6 Na^+Mt wt.%, respectively (Table 2). These results were attributed to the barrier

mechanism which has been observed and reported previously in flame-retardant polymer nanocomposites [63, 64]. According to "14 C.F.R. standard," the average burn length must not exceed 15.2 cm. Therefore, leather with Na^+Mt (3 and 6 wt.%) are suitable for upholstery uses in the aeronautic industry.

Mechanical properties, tensile strength, strain at break, and tear strength of reference leather and leather with Na^+Mt samples were also evaluated. According to Table 3, tensile strength and tear strength were enhanced by using 1 and 3 wt.% of Na^+Mt which evidences the reinforcing effect of Na^+Mt interacting physically with the leather, even at these low contents.

Na^+Mt content [wt.%]	Burning length [cm]
0	16.4 (±0.9)
1	14.3 (±0.7)
3	13.3 (±0.5)
6	13.4 (±1.1)

Table 2. Burning length of leather samples.

Na^+Mt content [wt.%]	Tensile strength [MPa]	Tear strength [N]	Strain at break [%]
0	16.5 (±0.7)	79 (±3.0)	51 (±1)
1	22.5 (±0.4)	94 (±1.0)	51 (±2)
3	22.8 (±0.8)	85 (±5.0)	41 (±1)
6	17.0 (±0.8)	85 (±5.0)	34 (±1)

Table 3. Mechanical properties of leather samples.

In conclusion, morphology, thermal stability, and flame-retardant and mechanical properties were studied on semifinished leather using Na^+Mt particles. It was found that by using 3 wt.% of Na^+Mt present during retanning process of leather, flame–retardant, and mechanical properties are improved. A semifinished leather suitable for aeronautic industry as upholstery product was obtained.

3. Clay minerals as flame-retardant additives on polymer blends

In the last decades, clay minerals have demonstrated to be efficient nontoxic flame-retardant systems to produce polymer composites [63, 65]. Different mechanisms have been proposed on how clay minerals act as flame retardants, and these mechanisms mainly vary depending on the polymer matrix. In some cases, clay mineral may change the polymer thermal degradation process, causing cross-linking, or promote the formation of a carbonaceous char layer

on the surface of the burning material, which acts as an insulating barrier [66]. Currently, the flame-retardant properties of clay minerals have become a very common topic for industrial and academic research due to their versatility and advantages, such as efficiency, environment friendly, and good impact on mechanical properties, with respect to traditional flame-retardant additives [67].

3.1. High-impact polystyrene

High-impact polystyrene (HIPS) is a widely used polymer in different industry fields due to its high-impact resistance. However, this polymer is highly flammable when exposed to fire, since it shows a low char-forming tendency during combustion process due to its chemical structure: aliphatic groups connected to aromatic moieties [68]. To improve HIPS flame-retardant properties, agents formulated from halogenated compounds have been used traditionally [69, 70]. Unfortunately, these compounds form highly toxic vapors during the combustion process.

Sanchez-Olivares et al. [19] analyzed in detail the fire behavior of high-impact polystyrene (HIPS) using Na^+Mt intercalated with triphenyl phosphite (Tri-Ph) as halogen-free flame-retardant additive. Intercalated sodium montmorillonite (Na^+Mt/Tri-Ph) was obtained by mixing Na^+Mt and Tri-Ph (viscous liquid) at 1:1 ratio, along with stirring at 90–105°C to render a homogenous slurry. Thermogravimetry analysis was carried out in order to evaluate the Tri-Ph intercalation in the Na^+Mt gallery. Na^+Mt, Tri-Ph, and Na^+Mt/Tri-Ph samples were evaluated. It was found that when Tri-Ph is intercalated in Na^+Mt, the thermal stability is higher than for pure Tri-Ph. A conical twin-screw intermeshing counter-rotating extruder (TS) and a single-screw extruder adapted with a static mixing die (SS-MD), which had conical compression and decompression sections to produce extensional flows, were employed in order to evaluate Na^+Mt/Tri-Ph dispersion effect on fire behavior of HIPS. About 5 phr of Na^+Mt/Tri-Ph were added to HIPS during TS and SS-MD extrusion process. The injection molding method was carried out to obtain HIPS–Na^+Mt/Tri-Ph specimens to evaluate fire behavior. Intercalation degree of samples Na^+Mt/Tri-Ph, HIPS-Na^+Mt/Tri-Ph_TS, and HIPS-Na^+Mt/Tri-Ph_SS-MD was studied using X-ray diffraction analysis. The Na^+Mt/Tri-Ph X-ray pattern showed the characteristic peak of mineral clay in 2-10 degree at 2 theta scale diffraction (Cu-K_αX-raysource, λ= 1.540562 Å). However, the HIPS-Na^+Mt/Tri-Ph_TS and HIPS-Na^+Mt/Tri-Ph_SS-MD patterns did not show that peak, which was attributed to the effect of clay mineral intercalation in the polymer matrix caused by the shear forces during mixing.

Combustion behavior of HIPS, HIPS-Na^+Mt/Tri-Ph_TS and HIPS-Na^+Mt/Tri-Ph_SS-MD samples was studied through limited oxygen index (LOI), UL94 vertical position, and cone calorimetric tests. According to limited oxygen index results, LOI was slightly increased for HIPS-Na^+Mt/Tri-Ph_SS-MD sample, from 18.8% (HIPS) to 19.6%with respect to the LOI percent of HIPS-Na^+Mt/Tri-Ph_TS sample, it was 19.2% which is very close to the HIPS value (18.8%). LOI results indicated that fire behavior HIPS-Na^+Mt/Tri-Ph under controlled atmosphere is slightly improved using single-screw extruder/static mixing die (SS-MD); probably compression and decompression zones (extensional flow) contributed to improve Na^+Mt/Tri-Ph dispersion and distribution. With respect to UL94-V results, no differences on flammability of the HIPS-Na^+Mt/Tri-Ph_TS and HIPS-Na^+Mt/Tri-Ph_SS-MD samples were observed with

respect to HIPS. These results provide evidence that the extrusion process does not substantially influence the flammability properties of the sample HIPS-Na^+Mt/Tri-Ph. Nevertheless, the fire behavior under forced combustion in cone calorimeter test showed differences depending on the extrusion process. Fig. 10 depicts the heat release rate versus time to ignition curves of HIPS, HIPS-Na^+Mt/Tri-Ph_TS, and HIPS-Na^+Mt/Tri-Ph_SS-MD samples. The peak heat release rate (pkHRR) is reduced about 13% with respect to that of HIPS when the single-screw process with the static mixing die (SS-MD) is used. On the contrary, when the twin-screw extrusion process (TS) is employed, the increase of pkHRR is about 3%. Good dispersion and distribution of clay mineral (Na^+Mt) in the polymer matrix was achieved by the use of a static mixer die. When clay mineral is well dispersed and distributed in the polymer matrix, it probably acts as a barrier for the combustion process by forming a protective char layer and reducing the heat release rate. Good dispersion of particles in the polymer matrix is associated with significant changes in the pkHRR values. Actually, poor dispersion of particles at the micrometer level has been reported to be associated with an increase in the value of the pkHRR[17].

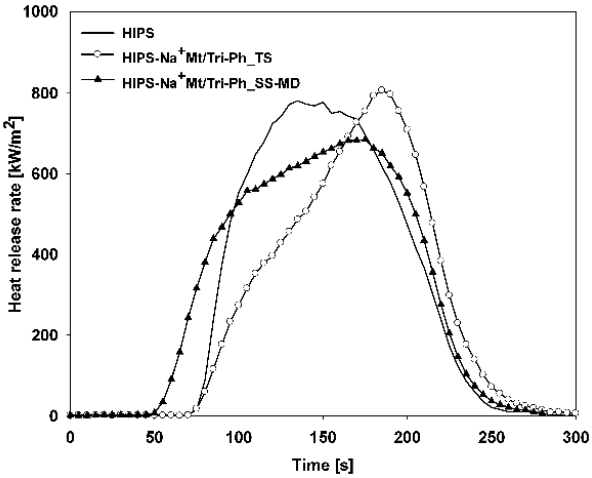

Figure 10. Heat release rate with respect to ignition time for the HIPS, HIPS-Na^+Mt/Tri-Ph_TS, and HIPS-Na^+Mt/Tri-Ph_SS-MD samples.

Finally, the use of a static mixing die placed at the end of a single-screw extruder improves clay minerals distribution and reduces the peak heat release rate according to the cone calorimeter test; the results are even better than those obtained by using a twin-screw extrusion process. An important relation for HIPS blends between clay dispersion and fire-retardant properties was found; i.e., the peak heat release rate decreases when good clay dispersion is achieved.

3.2. Polypropylene

The intumescent systems have been extensively studied as flame-retardant agents on polymers materials. The results have showed very good effectivity [71-72]. However, in order to achieve

these results, it is necessary to use a large amount of these additives (>30%). These high concentrations cause great problems during the processing of these materials and affect negatively their mechanical properties. A suggested technique for obtaining a good dispersion and distribution of the dispersed phase particles in polymer composites is the on-line application of ultrasonic waves during the extrusion process. Important advantages such as the distribution and dispersion of particles of carbon nanotubes and various clay minerals to the nanometric size have been achieved by using this process [73-76].The processing of flame-retardant intumescent systems together with modified clay mineral was studied in detail. Extrusion processes, such as twin screw (TS) and single screw, adapted with a special static mixer die with ultrasound application (SS-MDU) were considered. It was found that process conditions influence clay mineral dispersion which has a remarkable impact on the flame-retardant and mechanical properties [20]. Sodium bentonite was modified by an ion exchange method, using a mono-chlorohydrated amino acid to obtain organically modified clay (organoclay, referred to as OCLAY). An intumescent system, composed of pentaerythritol, melamine, and ammonium polyphosphate, was used as a flame-retardant compound. Polypropylene, OCLAY, and the intumescent system were processed by both extrusion processes mentioned (TS and SS-MDU). Table 4 discloses the composition of the materials.

Sample identification	Extrusion process	IFR [phr]	OCLAY [phr]
PP-IFR 30	Twin screw	30	0
PP-IFR 21	Twin screw	21	0
PP-IFR 21_C1	Twin screw	21	1
PP-IFR 30-US	Single screw Ultrasound	30	0
PP-IFR 21-US	Single screw Ultrasound	21	0
PP-IFR 21_C1-US	Single screw Ultrasound	21	1

Table 4. Materials composition based on PP.

The morphological study by scanning electron microscopy (SEM) revealed that when the materials are processed by SS-MDU extrusion, an important improvement on IFR (Intumescent Flame Retardant) particles dispersion and distribution is achieved. All materials processed by TS extrusion, PP-IFR 30, PP-IFR 21, and PP-IFR 21_C1, presented IFR agglomerates of about 10–30 μm. This confirms that by using the traditional extrusion process, it is difficult to disperse and distribute IFR particles. On the contrary, all the materials processed by the SS-MDU extrusion (PP-IFR PP-30-US, PP-IFR 21-US, and PP-IFR 21_C1-US) presented better dispersion and distribution of IFR particles in comparison with those processed by the TS extrusion, since IFR particles of 1–3 μm were observed in the former systems.

According to flame-retardant properties evaluated by UL94 vertical position standard of the studied materials (Table 5), the addition of OCLAY shows an important effect, depending on

http://dx.doi.org/10.5772/61588

the extrusion process employed. When the materials are compounded with high IFR content (30 phr: parts per hundred parts of resin), V0 classification was achieved regardless of extrusion processes (TS or SS-MDU). However, when IFR content is reduced to 21 phr, no V0 classification was observed. These results confirm that traditional flame-retardant additives must be added at high contents in order to obtain the desired effect. Nevertheless, when 1 phr of OCLAY is added, even at low IFR content (21 phr), V0 classification was obtained by using the SS-MDU process. These results are related to an improved dispersion and distribution of IFR and also to the effect of OCLAY, which was probably exfoliated.

Sample identification	UL94-V ating
PP	Fail
PP-IFR 30	V0
PP-IFR 21	Fail
PP-IFR 21_C1	Fail
PP-IFR 30-US	V0
PP-IFR 21-US	Fail
PP-IFR 21_C1-US	V0

Table 5. Flame retardant properties of PP materials.

Table 6 discloses the mechanical properties of the PP materials. The results showed clearly that OCLAY and ultrasound applications have a good impact on the mechanical properties of the PP-IFR materials, since the PP-IFR 21_C1-US sample showed better Izod impact resistance and strain at break with respect to traditional flame-retardant systems (PP-IFR 30). The Izod impact resistance increased from 73 to 89 J/m, and the strain at break from 17 to 115%, respectively. These results were attributed to an improved dispersion of particles (IFR and OCLAY), as small particles inhibit the fracture propagation by acting as stress concentrators.

Sample identification	Izod impact resistance [J/m]	Strain at break [%]
PP	175	163
PP-IFR 30	73	17
PP-IFR 21	65	98
PP-IFR 21_C1	67	39
PP-IFR 30-US	84	34
PP-IFR 21-US	124	95
PP-IFR 21_C1-US	89	115

Table 6. Mechanical properties of PP materials.

To sum up, it has been demonstrated that clay mineral (OCLAY) has a remarkable effect on flame-retardant and mechanical properties in the PP matrix. With the use of clay mineral and a special extrusion process, the content of traditional flame retardant is reduced from 30 to 21 phr to obtain a V0 classification, according to the UL94 vertical position. Moreover, Izod impact resistance and strain at break were improved with respect to systems with high flame-retardant additives content (30 phr).

3.3. High-density polyethylene

The use of clay minerals as flame-retardant additives for industrial applications is highly attractive due to the synergistic effect on flame-retardant properties of polymer materials achieved by the combination of clay minerals and traditional flame-retardant additives. This combination allows obtaining the right properties for industrial applications with less flame-retardant additive contents (loads).Also, the cost of the final material may be cheaper than traditional flame-retardant systems [77]. The use of sodium bentonite (chemically modified) at specific content along with high-density polyethylene (HDPE) demonstrated an important reduction in aluminum trihydroxide content (lower about 40%) to reach the optimal V0 UL94 classification. Moreover, mechanical properties were improved with respect to common flame-retardant HDPE composite [21]. HDPE, modified bentonite (OCLAY), aluminum trihydroxide (ATH), and zinc borate (ZnB) were processed in a twin-screw counter-rotating extruder (TS). Alternatively, a single-screw extruder was coupled to a static mixer die, which promotes extensional flow, assisted by piezoelectric elements to generate ultrasonic waves (SS-US). Table 7 discloses the HDPE materials composition.

Sample identification	Extrusion process	ATH [phr]	ZnB [phr]	OCLAY [phr]
PE-50ATH	Twin screw	50	0	0
PE-30ATH-3ZnB	Twin screw	30	3	0
PE-30ATH-3ZnB-C1	Twin screw	30	3	1
PE-30ATH-3ZnB-C2	Twin screw	30	3	2
PE-30ATH-3ZnB/US	Single screw ultrasound	30	3	0
PE-30ATH-3ZnB-C1/US	Single screw ultrasound	30	3	1
PE-30ATH-3ZnB-C2/US	Single screw ultrasound	30	3	2

Table 7. Materials composition based on HDPE.

The morphological study by scanning electron microscopy (SEM) showed that the SS-US extrusion process is a very good method to improve the dispersion and distribution of ATH

particles. Agglomerates of the ATH particles (around 1–3 μm) were observed when the materials were processed by TS. It illustrates the problem to achieve an adequate level of dispersion and distribution of the additives with high ATH concentration. On the contrary, when the materials were processed by SS-US, the ATH particles were reduced in size and no agglomerates were observed. Aluminum elemental analysis was carried out in order to confirm the dispersion and distribution level of ATH.

Table 8 discloses flame-retardant properties evaluated by UL94-V. According to results, the materials obtained with high flame-retardant additive content (50 phr of ATH) render an optimum V0 classification. This result is not surprising considering that, at high concentrations, the flame-retardant additives are very effective. However, when the ATH additive content is reduced (from 50 phr to 30 phr), no V0 rating is reached, even with the additives combination of ZnB (3 phr) and the addition of different OCLAY content (1 and 2 phr). Nevertheless, when the same materials, PE-30ATH-3ZnB/US, PE-30ATH-3ZnB-C1/US, and PE-30ATH-3ZnB-C2/US, are processed under the SS-US extrusion, V2, V2 and V0 ratings, respectively, are obtained. These results demonstrated that a specific content of OCLAY (2 phr) and its good dispersion (probably at the nanometric scale), as well as an efficient dispersion and distribution of the additives (ATH and ZnB) with the help of an on-line ultrasound system (SS-US) rendered an optimized flame-retardant HDPE.

Sample identification	UL94-V rating
HDPE	Fail
PE-50ATH	V0
PE-30ATH-3ZnB	Fail
PE-30ATH-3ZnB-C1	Fail
PE-30ATH-3ZnB-C2	Fail
PE-30ATH-3ZnB/US	V2
PE-30ATH-3ZnB-C1/US	V2
PE-30ATH-3ZnB-C2/US	V0

Table 8. Flame retardant properties of HDPE materials.

Mechanical properties of the materials based on HDPE are disclosed in Table 9. One of the main problems in flame-retardant polymers is the negative effect on mechanical properties when a high load of additives is used. This is clearly observed in Table 9, where the material with highest additive content (50 phr) displayed poor mechanical properties: Izod impact resistance and strain at break. However, when the materials are extruded with the SS-US, the mechanical properties are greatly improved, in particular with the addition of OCLAY (samples PE-30ATH-3ZnB-C1/US and PE-30ATH-3ZnB-C2/US).

Sample identification	Izod impact resistance [J/m]	Strain at break [%]
HDPE	153	>500
PE-50ATH	53	43
PE-30ATH-3ZnB	52	200
PE-30ATH-3ZnB-C1	53	83
PE-30ATH-3ZnB-C2	49	52
PE-30ATH-3ZnB/US	63	191
PE-30ATH-3ZnB-C1/US	70	350
PE-30ATH-3ZnB-C2/US	85	210

Table 9. Mechanical properties of HDPE materials.

The use of on-line ultrasound application with a special mixer die, effectively reduced the size of ATH particles (<1 μm) and improved the particle dispersion and distribution within the polymer matrix. The improvement of the dispersion of the flame-retardant additives attained by the combination of ultrasound and mixing die had a positive effect in the flame-retardant properties. Most of the obtained materials were classified as UL94-V2, and a V0 rating was achieved with the addition of 2 phr of OCLAY. Mechanical properties (Izod impact resistance and strain at break) were also improved. An optimal flame-retardant HDPE composite was obtained by reducing the ATH content from 50 phr (typical high concentration) to 30 phr (21.5 wt.%).

Author details

Guadalupe Sanchez-Olivares[1*], Fausto Calderas[1], Luis Medina-Torres[2], Antonio Sanchez-Solis[3], Alejandro Rivera-Gonzaga[4] and Octavio Manero[3]

*Address all correspondence to: gsanchez@ciatec.mx, fcalderas@ciatec.mx

1 CIATEC, A. C., León, Gto., Mexico

2 Facultad de Química, Universidad Nacional Autónoma de México, Ciudad Universitaria, México D.F., Mexico

3 Instituto de Investigaciones en Materiales, Universidad Nacional Autónoma de México, Ciudad Universitaria, México D.F., Mexico

4 Instituto de Ciencias de la Salud, Universidad Autónoma del Estado de Hidalgo, San Agustín Tlaxiaca, Hgo., Mexico

References

[1] Murray H. Applied clay mineralogy today and tomorrow. Clay Minerals. 1999;34:39–49.

[2] Bergaya, F., Lagaly, G. Chapter 1: Clays, Clay Minerals, and Clay Science, Developments in Clay Science. In: Bergaya et al., editor. Handbook of clay science. Amsterdam, The Netherlands: Elsevier; 2006. pp. 1–18

[3] Camargo P., Satyanarayana K., Wypych F. Nanocomposites: Synthesis, Structure, Properties and New Application Opportunities. Materials Research. 2009;12:1–39.

[4] Alateyah A., Dhakai H., Zhang Z. Processing, Properties, and Applications of Polymer Nanocomposites Based on Layer Silicates: A Review. Advances in Polymer Technology. 2013;32:21368.

[5] Zare Y. Recent progress on preparation and properties of nanocomposites from recycled polymers: A review. Waste Management. 2013;33:598–604.

[6] Mittal V. Polymer Layered Silicate Nanocomposites: A Review. Materials. 2009;2:992–1057.

[7] Pavlidou S., Papaspyrides C. A review on polymer–layered silicate nanocomposites.. Progress in Polymer Science. 2008;33:1119–1198.

[8] Ray S., Okamoto M. Polymer/layered silicate nanocomposites: a review from preparation to processing. Progress Polymer Science. 2003;28:1539–1641.

[9] Alexandre M., Dubois P. Polymer-layered silicate nanocomposites: preparation, properties and uses of a new class of materials. Materials Science and Engineering. 2000;28:1–63.

[10] Konta J. Clay and man: Clay raw materials in the service of man. Applied Clay Science. 1995;10:275–335.

[11] Rahmat M., Hubert P. Carbon nanotube–polymer interactions in nanocomposites: A review. Composites Science and Technology. 2014;72:72–84.

[12] Hu K., Kulkarni D., Choi I., Tsukruk V. Graphene-polymer nanocomposites for structural and functional applications. Progress in Polymer Science.. 2014;39:1934–1972.

[13] Mittal G., Dhand V., Rhee K., Park S., Lee W. A review on carbon nanotubes and graphene as fillers in reinforced polymer nanocomposites. Journal of Industrial and Engineering Chemistry. 2015;21:11–25.

[14] Rivera-Gonzaga A., Sanchez-Solis A., Sanchez-Olivares G., Calderas F., Manero O. Unsaturated polyester-clay slurry nanocomposites. Journalof Polymer Engineering. 2012;32:1–5.

[15] Calderas F., Herrera-Valencia E. E., Sanchez-Solis A., Manero O., Medina-Torres, L., Renteria A., Sanchez-Olivares G. On the yield stress of complex materials. Korea-Australia Rheology Journal. 2013;25:233–242.

[16] Sanchez-Olivares G., Sanchez-Solis A., Calderas F., Medina-Torres L., Manero O., Di Blasio, A. Alongi J. Sodium montmorillonite effect on the morphology, thermal, flame retardant and mechanical properties of semi-finished leather. Applied Clay Science. 2014;102:254–260.

[17] Sanchez-Olivares G. Sanchez-Solis A., Manero O. Effect of montmorillonite clay on the burning rate of high-impact polystyrene. International Journal of Polymeric Materials and Polymeric Biomaterials. 2008;57:245–257.

[18] Calderas F., Sanchez-Olivares G., Herrera-Valencia E. E., Sanchez-Solis A., Manero O. Chapter 6: PET-MMT and PET-PEN-MMT Nanocomposites by Melt Extrusion. In: Boreaddy S. R. Reddy, editor. Advances in Nanocomposites-Synthesis, Characterization and Industrial Applications. Rijeka, Croatia: Intech; 2011. pp. 101–120.

[19] Sanchez-Olivares G., Sanchez-Solis A., Manero O. Study on the combustion behavior of high impact polystyrene nanocomposites produced by different extrusion processes. eXPRESS Polymer Letters. 2008;2:569–578.

[20] Sanchez-Olivares G., Sanchez-Solis A., Calderas F., Medina-Torres L., Herrera-Valencia E.E., Rivera-Gonzaga A., Manero O. Extrusión with ultrasound applied on intumescent flame retardant polypropylene. Polymer Engineering and Science. 2013;53[20]:2018–2026.

[21] Sanchez-Olivares G., Sanchez-Solis A., Calderas F., Medina-Torres L., Herrera-Valencia E. E., Castro-Aranda J. I., Manero O., Di Blasio A., Alongi J. Flame retardant high density polyethylene optimized by on-line ultrasound extrusion. Polymer Degradation and Stability. 2013;98:2153–2160.

[22] Ahmad K., Pan W. Microstructure-toughening relation in alumina based multiwall carbon nanotube ceramic composites. Journal of the European Ceramic Society. 2015;35:663–671.

[23] Mukherjee S., Kundu B., Chanda A., Sen S. Effect of functionalisation of CNT in the preparation of HAp–CNT biocomposites. Ceramics International. 2015;41:3766–3774.

[24] Fan Y., Igarashi G., Jiang W., Wang L., Kawasaki A. Highly strain tolerant and tough ceramic composite by incorporation of graphene. Carbon. 2015;90:274–283. DOI: 10.1016/j.carbon.2015.04.029

[25] Harvey C., Murray H. Industrial clays in the 21st century: A perspective of exploration, technology and utilization. Applied Clay Science. 1997;11:285–310.

[26] Viseras C., Aguzzi C., Lopez-galindo A. Uses of clay minerals in semisolid health care and therapeutic products. Applied Clay Science. 2007;36:37–50.

[27] Aguzzi C., Sanchez-Espejo R., Cerezo P., Machado J., Bonferoni C., Rossi S., Salcedo I., Viseras C. Networking and rheology of concentrated clay suspensions "matured" in mineral medicinal water. International Journal of Pharmaceutics. 2013;453:473–479.

[28] Cruz N., Peng Y., Farrokhpay S., Bradshaw D. Interactions of clay minerals in copper–gold flotation: Part 1 – Rheological properties of clay mineral suspensions in the presence of flotation reagents. Minerals Engineering. 2013;50–51:30–37.

[29] Paineau E., Michot L., Bihannic I., Baravian C. Aqueous Suspensions of Natural Swelling Clay Minerals. 2. Rheological Characterization. Langmuir. 2011;27:7806–7819.

[30] Cheng D.C.H. Yield stress: A time-dependent property and how to measure it. Rheologica Acta. 1986;25:542–554.

[31] Evans I.D. Letter to the editor: On the nature of the yield stress. Journal of Rheology. 1992;36:1313–1316.

[32] Barnes H.A. The yield stress—a review —everything flows?. Journal of Non-Newtonian Fluid Mechanics. 1999;81:133–178.

[33] Bingham E.C. Fluidity and Plasticity. New York: McGraw-Hill; 1922.

[34] Herschel W.H.,Bulkley R. Konsistenzmessungen von Gummi-Benzol-Loesungen. Kolloid Zeitschrift. 1926;39:291–300.

[35] Papanastasiou T.C. Flows of materials with yield. Journal of Rheology. 1987;31:385–404.

[36] Houlsby G.T., Puzrin A. M. Rate-dependent plasticity models derived from potential functions. Journal of Rheology. 2002;46:113–126.

[37] Isayev A., Fan X. Viscoelastic plastic constitutive equation for flow of particle filled polymers. Journal of Rheology. 1990;34:35–54.

[38] SaramitoP. A new constitutive equations for elastoviscoplastic fluid flows. Journal of Non-Newtonian Fluid Mechanics. 2007;145:1–14.

[39] Saramito P. A new elastoviscoplastic model based on the Herschel-Bulkley viscoplastic model. J. Non-Newtonian Fluid Mech. 2009;158:154–161.

[40] Bautista F., De Santos J.M., Puig J.E.,Manero O. Understanding thixotropic and antithixotropic behavior of viscoelastic micellar solutions and liquid crystalline dispersions. The model. Journal of Non-Newtonian Fluid Mechanics. 1999;80:93–113.

[41] Soltero J, Puig J., Manero O. Rheology of Cetyltrimethylammonium p-Toluenesulfonate-Water System. 3, Nonlinear Viscoelasticity. Langmuir. 1999;15:1604–1612.

[42] Bautista F., Soltero J.F.A., Macias E.R., Puig J.E., Manero O. Thermodynamics approach and modeling of Shear-Banding Flow of Wormlike Micelles. Journal of Physical Chemistry B. 2002;106:13018–13026.

[43] Bautista F., Perez-Lopez J. H., Garcia J. P., Puig J.E., Manero O. Stability analysis of shear banding flow with the BMP model. Journal of Non-Newtonian Fluid Mechanics. 2007;144:160–169.

[44] Herrera EE, Calderas F, Chávez AE, Manero O, Mena B. Effect of random longitudinal vibration pipe on the Poiseuille-flow of a complex liquid. RheologicaActa. 2009;48:779–800.

[45] Herrera EE, Calderas F, Chavez AE, Manero O. Study of the pulsating flow of a worm-like micellar solution. Journal of Non-Newtonian Fluid Mechanics. 2010;165:174–183.

[46] Manero O., Perez-Lopez J. H., Escalante J. I., Puig J.E., Bautista F. A thermodynamic approach to rheology of complex fluids: The generalized BMP model. Journal of Non-Newtonian Fluid Mechanics. 2007;146:22–29.

[47] Escalante J.I., Macias E.R., Bautista F., Pérez-López J.H., Soltero J.F.A., Puig J.E., Manero O. Shear-banded flow and transient Rheology of cationic wormlike Micellar solutions. Langmuir. 2003;19:6620–6626.

[48] Escalante J.I., Escobar D., Macias E.R., Perez-Lopez J.H., Bautista F., Mendizabal E., Puig J.E., Manero O. Effect of a hydrotope on the viscoelastic properties of polymer-like micellar solutions. Rheologica Acta. 2007;46:685–691.

[49] Moreno L., Calderas F., Sanchez-Olivares G., Medina-Torres L., Sanchez-Solis A., Manero O. Effect of cholesterol and triglycerides levels on the rheological behavior of human blood. Korea-Australia Rheology Journal. 2015;27:1–-10.

[50] Casson N. A flow equation for pigment oil suspensions of printing type ink. In: Mill C. C, editor. Rheology of disperse systems. Oxford, U.K: Pergamon Press; 1959. pp. 84–104.

[51] Fu X., Qutubuddin S. Synthesis of unsaturated polyester-clay nanocomposites using reactive organoclays. Polymer Engineering and Science. 2004;44:345–351.

[52] Mironi-Harpaz I., Narkis M., Siegmann A. Nanocomposite system based on unsaturated polyester and organoclay. Polymer Engineering and Science. 2005;45:174–185.

[53] Suh D.J., Lim Y.T., Park O.O. The property and formation of unsaturated polyester-layered silicate nanocomposites depending on fabrication methods. Polymer. 2000;41:8557–8563.

[54] Inceoglu A.B., Yilmazer U. Synthesis and mechanical properties of unsaturated polyester based nanocomposites. Polymer Engineering and Science. 2003;43:661–669.

[55] Salahuddin N.A. Layered silicate/epoxy nanocomposites: synthesis, characterization and properties. Polymers for Advanced Technologies. 2004;15:251–259.

[56] Bongiovanni R., Mazza D., Roncheti S., Turcato E.A. The influence of water on the intercalation of epoxy monomers in Na-montmorillonite. Journal of Colloid and Interface Science. 2006;296:515–519.

[57] Hasegawa N., Okamoto H., Kato M., Usuki A., Sato N. Nylon 6/Na-montmorillonite nanocomposites prepared by compounding Nylon 6 with Na-montmorillonite slurry. Polymer. 2003;44:2933–2937.

[58] Wang K., Wang L., Wu J. S., Chen L., He C. B. Preparation of exfoliated epoxy/clay nanocomposites by "slurry compounding": process and mechanisms. Langmuir. 2005;21:3613–3618.

[59] Wang K., Wu J. S., Chen L., Toh M.L., He C. B., Yee A.F. Epoxy nanocomposites with highly exfoliated clay: mechanical properties and fracture mechanisms. Macromolecules. 2005;38:788–800.

[60] Chen Y., Fan H., Shi B. Nanotechnologies for leather manufacturing: a review. Journal of the American Leather Chemists Association. 2011;106:260–273.

[61] Budrugeac P., Miu L., Bocu V., Wortman F.J., PopescuC. Thermal degradation of collagen-base materials that are supports of cultural and historical objects. Journal of Thermal Analysis and Calorimetry. 2003;72:1057–1064.

[62] Kaminska A., Sionkowska A. The effect of UV radiation on the thermal parameters of collagen degradation. Polymer Degradation and Stability. 1993;51:15–18.

[63] Gilman J.W. Flammability and thermal stability studies of polymer layered-silicate (clay) nanocomposites. Applied Clay Science. 1999;15:31–49.

[64] Schartel B., Bartholmai M., KnollU. Some comments on the main fire retardancy mechanisms in polymer nanocomposites. Polymers for Advanced Technologies. 2006;17:772–777.

[65] Kiliaris P., Papaspyrides C.D. Polymer/layered silicate (clay) nanocomposites: An overview of flame retardancy. Progress in Polymer Science. 2010;35:902–958.

[66] Gilman J.W. Flame retardant mechanism of polymer-clay nanocomposites. In: Morgan, A. B. and Wilkie, C.A, editors. Flame retardant polymer nancomposites. Hoboken, New Jersey: John Wiley and Sons; 2007. pp. 67–83.

[67] Alongi J., Carosio F., Malucelli G. Current emerging techniques to impart flame retardancy to fabrics: An overview. Polymer Degradation and Stability. 2014;106:138–149.

[68] Krevelen Van D. W., Nijenhuis te K. Properties of Polymers. 4th ed. Amsterdam: Elsevier; 2009. pp. 772–774.

[69] Utevski L., Scheinker M., Georlette P., Lach S. Flame retardancy in UL-94 V-0 and in UL-94 5VA high impact polystyrene. Journal of Fire Sciences. 1997;15:375–389.

[70] Chin-Ping Y., Biing-Shiow S. Effect of tetrabromobisphenol. A diallyl ether on flame retardancy of high impact strength polystyrene. Journal of Applied Polymer Science. 1989;37:3185–3194.

[71] Camino G., Costa L., Martinasso G. Intumescent fire-retardant systems. Polymer Degradation and Stability. 1989;23:359–376.

[72] Horacek H., Pieh S. The importance of intumescent systems for fire protection of plastic materials. Polymer International. 2000;49:1106–1114.

[73] Peng B., Wu H., Bao W., Guo S., Chen Y., Huang H., Chen H., Lai S. Y., Jow J. Effects of ultrasound on the morphology and properties of propylene-based plastomer/nanosilica composites. Polymer Journal. 2011;43:91–96.

[74] Isayev A. I., Kumar R., Lewins T. M. Ultrasound assisted twin screw extrusion of polymer-nanocomposites containing carbon nanotubes. Polymer. 2009;50:250–260.

[75] Li J., Zhao L. J., Guo S. Y. Ultrasound assisted development of structure and properties of polyamide 6/montmorillonite nanocomposites. Journal of Macromolecular Science, Part B: Physics. 2007;46:423–439.

[76] Lapshin S., Swain S. K., Isayev A. I. Ultrasound aided extrusion process for preparation of polyolefin-clay nanocomposites. Polymer Engineering and Science. 2008;48:1584–1591.

[77] Beyer G. Flame retardant properties of organoclays and carbon nanotubes and their combination with alumina trihydrate. In: Morgan A. B., Wilkie C.A, editors. Flame retardant polymer nanocomposites. Hoboken, New Jersey: John Wiley and Sons, Inc; 2007. pp. 164–177.